Spontaneous Fission of Pu^{240}: Comparison with the Slow-Neutron-Induced Fission of Pu^{239}†

Jayashree Toraskar and E. Melkonian
Columbia University, New York, New York 10027
(Received 7 October 1970)

Fission-fragment mass and kinetic energy distributions have been obtained for the spontaneous fission of Pu^{240} and compared with those for the thermal-neutron-induced fission of Pu^{239} reported previously. Surface-barrier detectors were used for the simultaneous measurements of energies of both the fission fragments. Absolute fragment energies were calculated by using mass-dependent pulse-height energy relations. The measured average total kinetic energies were found to be 177.3 ± 1.5 MeV and 173.0 ± 1.5 MeV for the spontaneous and the induced fission, respectively, and the average pre-neutron total kinetic energies were 178.9 ± 1.5 MeV and 175.2 ± 1.5 MeV, respectively. The measured mass distribution for the spontaneous fission appears to be significantly different in shape from that for the induced fission.

INTRODUCTION

In spontaneous fission, the excitation energy of the fissioning nucleus is zero so that the characteristics of spontaneous fission should provide basic information about the fission process. However, only the spontaneous fission of Cf^{252} has been studied extensively because the easily available nuclei such as thorium, uranium, and plutonium have very long half-lives against spontaneous fission, while most of the short-lived transplutonium elements are not yet available in properly purified form in sufficient amounts.

The spontaneous-fission characteristics of Pu^{240} are particularly important from another point of view also, that of comparison with the neutron-induced fission of Pu^{239}. It was suggested by Wheeler that the symmetric mass yield in a fission process depends on the spin state of the compound nucleus. The ground state of Pu^{239} has spin $\frac{1}{2}^+$ so that the compound nucleus formed by addition of a slow s-wave neutron has spin 0^+ or 1^+. By using resonance-energy neutrons, fission from the 0^+ state of the excited Pu^{240} compound nucleus can be studied. Comparison of the fission characteristics of this state with those of ground state should provide information about the effect of excitation energy on the fission process for the same spin state.

There are three other even-even compound nuclei, viz. U^{238}, Cm^{242} and Cf^{252}, which are spontaneously fissionable and which can also be formed in 0^+ and 1^+ spin states by addition of a slow neutron. However, the longer half-life of U^{238} (5.8×10^{15} years compared with 1.2×10^{11} years for Pu^{240}) makes the comparison difficult, while curium and Cf^{251} targets of high enough isotopic purity have not been readily available.

The single-fragment kinetic energy distribution from spontaneous fission of Pu^{240} was measured by Whitehouse and Galbraith,[1] and Segrè and Wiegand.[2] The first to measure the mass distribution for spontaneous fission of Pu^{240} and compare it with that for thermal-neutron-induced fission of Pu^{239} was Mostovaya.[3] She measured the energies of the complementary fragments by using a double-gridded ionization chamber. Her results indicate that for spontaneous fission, the peaks of the mass distribution are narrower than those for the induced fission of the same compound nucleus. Okolovitch and Smirenken[4] have used Mostovaya's data to conclude that the total kinetic energy released in spontaneous fission of Pu^{240} is 1.5 ± 0.5 MeV smaller than that released in the neutron-induced fission of Pu^{239}. Smith *et al.*[5] also measured the kinetic energies of fragments from spontaneous and induced fission of the Pu^{240} compound nucleus and found no energy difference for the two cases. The only other mass distribution measurement for the spontaneous fission of Pu^{240} was done by Laidler and Brown.[6] They measured fission yields of only 15 isotopes in the mass range 89–147 to obtain the post-neutron mass distribution, giving incomplete information about the detailed structure of the mass distribution.

The development of solid-state detectors with good pulse-height resolution and fast rise time has considerably improved the accuracy of energy measurement, making possible a better determination of energy distribution. We have measured the kinetic energies of both of the complementary fission fragments, using solid-state detectors, and have derived the mass distribution from these measurements. These results are compared with our previous measurements on the induced fission of Pu^{239} by beryllium-filtered neutrons.[7] A cold beryllium filter preferentially transmits neutrons with energies below 0.0052 eV so that the energy and mass distributions observed are primarily

those due to the negative energy level of the Pu^{240} compound nucleus. Experimental evidence indicates that this level has a 0^+ spin state. Thus we are comparing two 0^+ states with excitation energy difference of 6.3 MeV.

EXPERIMENTAL METHOD

The plutonium target used in the experiment had the following isotopic composition:

Pu^{239} 18.502%,

Pu^{240} 80.955%,

Pu^{241} 0.520%,

Pu^{242} 0.023%.

The target was prepared by vacuum evaporation of plutonium fluoride onto a 5-μ in.-thick nickel foil. The thickness of the deposit was ~20 $\mu g/cm^2$ on an area of ~200 mm^2.

Two heavy-ion surface-barrier detectors were arranged so that each one faced one side of the thin target mounted at the center of the fission chamber. Pulse heights from the coincident fission fragments were recorded. The details of the electronics are given elsewhere.[7]

The data were collected over a period of six weeks, and 1929 fission events were recorded. Pulses were fed into the system every 7.5 min during the data collection to check the stability of the system. In addition, system calibration was done after every 24 h to correct the data collected during that interval for the slight nonlinearity of the system. Absolute calibration of the detectors was done after the data collection with a thin Cf^{252} source. The energy and mass spectrum characteristics of the fission fragments from Cf^{252} indicated that the energy resolution of the whole system was good.

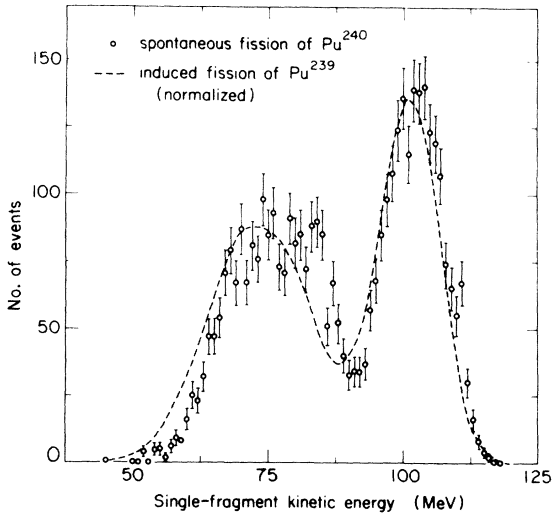

FIG. 1. Single-fragment kinetic energy distributions $N(E_1)$ for the spontaneous fission of Pu^{240} and the induced fission of Pu^{239} by beryllium-filtered neutrons.

DATA ANALYSIS

The measured pulse heights are linear functions of the fragment energies after neutron emission. No exact energy- and momentum-conservation relations can be used without considering the neutron emission from each fragment. We have used the following approximate relations to calculate the energies and masses of the two fragments:

$$\mu_1 E_1 = \mu_2 E_2 , \tag{1}$$

$$\mu_1 + \mu_2 = A , \tag{2}$$

$$E_K = E_1 + E_2 , \tag{3}$$

where E_1 and E_2 are the measured kinetic energies of the two complementary fragments, E_K is the total kinetic energy released in the fission event, and A is the mass number of the fissioning nucleus. Then

$$\mu_1 = AE_2/E_K . \tag{4}$$

Mass-dependent pulse-height energy relations[8] were used to calculate the energies E_1 and E_2 of the two fragments. Masses μ_1 were then calculated by using Eq. (4).

Average pre-neutron kinetic energies were obtained by using the following relation

$$\langle E_i \rangle = \left(1 - \frac{\langle \nu_i \rangle}{\langle \mu_i \rangle}\right) \langle E_i^* \rangle , \tag{5}$$

where i corresponds to light- or heavy- fragment group, $\langle E_i \rangle$ and $\langle \mu_i \rangle$ are the measured average kinetic energy and mass, and $\langle \nu_i \rangle$ is the average number of neutrons emitted by the light- or heavy-fragment group.

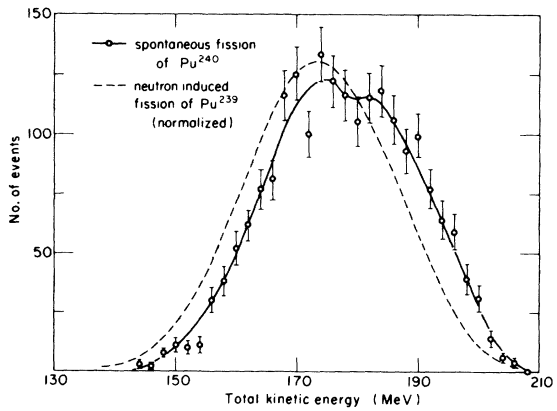

FIG. 2. Total kinetic energy distributions $N(E_K)$ for spontaneous fission of Pu^{240} and induced fission of Pu^{239} by beryllium-filtered neutrons.

RESULTS

The single-fragment kinetic energy distributions $N(E_1)$ for the spontaneous and the induced fission are shown in Fig. 1. Figure 2 shows the total kinetic energy distributions $N(E_K)$ for the two cases. The $N(E_K)$ distribution for the spontaneous case is asymmetric about the average value and shows a structure on the higher-energy side in contrast with that for the induced fission of Pu^{239}, which is fairly smooth and symmetric about its average values. Table I gives the average values of the various energies and the masses for the two cases. The measured average total kinetic energy for the spontaneous fission is 4.3 ± 2.1 MeV higher than that for induced fission. The average heavy- and light-fragment energies also show changes in the same direction. Note, however, that the change in the heavy-fragment energy is much larger than that in the energy of the light fragment. This may be the effect of a variation in the shape of the neutron-emission function with the excitation energy of the compound nucleus.

The pre-neutron average total kinetic energies for the spontaneous fission of Pu^{240} and the induced fission of Pu^{239} were found to be 178.9 ± 1.5 MeV and 175.2 ± 1.5 MeV, respectively. Thus the difference between the two pre-neutron energies is 3.7 ± 2.1 MeV which is smaller than the measured difference due to the fact that 2.12 average neutrons are emitted in the spontaneous fission of Pu^{240} compared with the 2.83 average neutrons emitted in the induced fission of Pu^{239}. Note that the quoted value of the pre-neutron total kinetic energy for the induced fission is slightly different than that given in the earlier paper. This is the result of using two different methods for neutron corrections, made necessary because experimental data on the variation of neutron number as a function of mass are not available for the spontaneous fission of Pu^{240}. However, for the comparison of two energies, this systematic error should cancel out.

TABLE I. Characteristics of the measured kinetic energy and mass distributions for the spontaneous fission of Pu^{240} and the neutron-induced fission of Pu^{239} (beryllium filter). All masses are in amu and energies in MeV. Uncertainties given are statistical and calibration errors.

Type	Induced fission of Pu^{239} (beryllium filter)	Spontaneous fission of Pu^{240}
$\langle \mu_L \rangle$	100.3 ± 1.0	102.5 ± 1.0
$\langle \mu_H \rangle$ [a]	139.5 ± 1.0	138.5 ± 1.0
$\langle E_L \rangle$	100.7 ± 1.2	101.7 ± 1.0
$\langle E_H \rangle$	72.3 ± 0.9	75.6 ± 1.0
$\langle E_K \rangle$	173.0 ± 1.5	177.3 ± 1.5
$\sigma(E_K)$	12.13	13.87
$\sigma(\mu_L)$	6.79	5.70
$\sigma(\mu_H)$	6.79	5.70

[a] Note that $\langle \mu_L \rangle$ and $\langle \mu_H \rangle$ were calculated by using masses of only one fragment and classifying them as light or heavy depending on whether the value was smaller or larger than 120. Poor statistics for the spontaneous fission gives $\langle \mu_L \rangle + \langle \mu_H \rangle = 241.0$ rather than 240 as would be the case if only $\langle \mu_L \rangle$ were calculated and the relation $\mu_L + \mu_H = A$ were used to obtain $\langle \mu_H \rangle$.

Figure 3 shows the mass distribution $N(\mu)$ derived from the spontaneous-fission data after reflection about mass 120. The normalized $N(\mu)$ distribution for the induced fission of Pu^{239} is superimposed for comparison. The shape of the spontaneous-fission mass distribution is significantly different from the one for the induced fission. In the case of spontaneous fission each mass peak appears very asymmetric about the average value. The fission yield drops very sharply near the symmetric mass division. The mass peaks are narrower and taller than those for the induced fission. Both peaks appear to have shifted toward mass 120.

The mass distribution $N(\mu)$ for the spontaneous fission and the variations of the average single-fragment and total kinetic energy as a function of mass μ are shown in Figs. 4 and 5. Note that the average kinetic energies differ significantly from those for the induced fission only in the regions of mass peaks. Figure 3 indicates that in these same regions, the fission yield is also significantly different for the two types of fission. Plotted in Figs. 6 and 7 are the rms widths of mass distributions corresponding to 5-MeV intervals of total kinetic energy distributions, and the average heavy-fragment masses for each of these mass distributions.

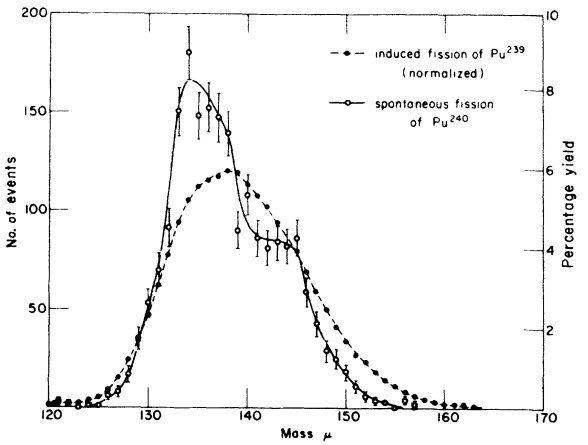

FIG. 3. Mass distribution $N(\mu)$ for spontaneous fission of Pu^{240} superimposed on the normalized mass distribution $N(\mu)$ for induced fission of Pu^{239} by beryllium-filtered neutrons.

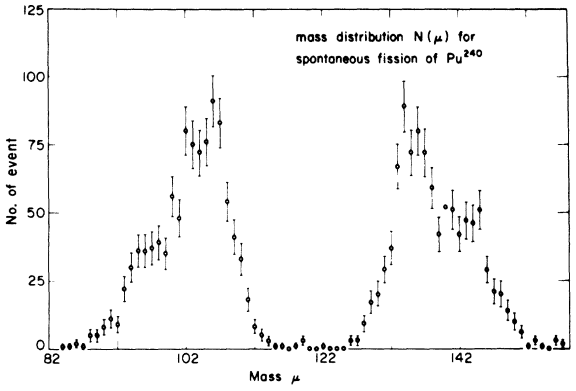

FIG. 4. Mass distribution $N(\mu)$ for the Pu^{240} spontaneous fission.

The widths of the mass distributions for the spontaneous fission are smaller than those for the induced fission and remain fairly constant in comparison with those for induced fission for which case the width of the mass distribution decreases with the increasing total kinetic energy. The average heavy-fragment masses show general agreement to within one mass unit.

DISCUSSION

Both the kinetic energy and the mass distributions in the case of the spontaneous fission of Pu^{240} are considerably different from those generally observed in the thermal-neutron-induced fission, so that particular attention was paid to the possibility of a large background fission rate. In particular the following processes were investigated: (1) spontaneous and neutron-induced fission of various plutonium isotopes present in the target; (2) contamination by elements with a short half-life

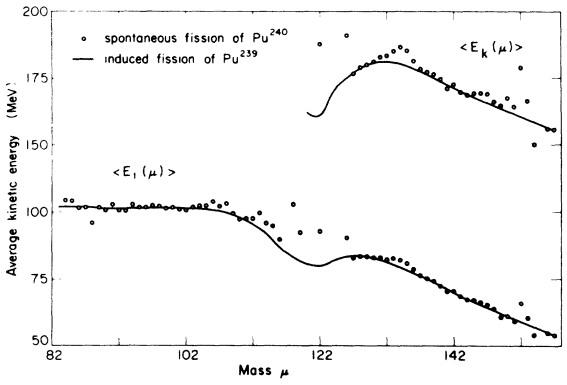

FIG. 5. Variations of measured average single-fragment and total kinetic energies as a function of mass μ for spontaneous fission of Pu^{240} and induced fission of Pu^{239} by beryllium-filtered neutrons. Smooth curves indicate quantities for the induced fission.

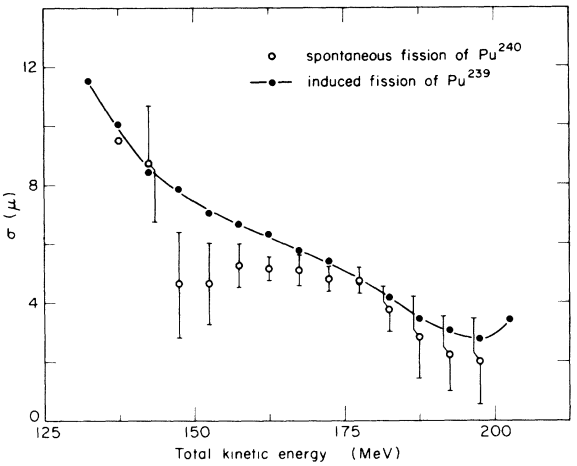

FIG. 6. rms widths $\sigma(\mu)$ of the mass distributions for each 5-MeV interval of total kinetic energy for spontaneous fission of Pu^{240} and induced fission of Pu^{239} by beryllium-filtered neutrons. Smooth curves indicate quantities for the induced fission.

against spontaneous fission; and (3) formation of isomeric states of various elements in the target by α bombardment:

(1) The calculations based on the measured neutron flux in the surroundings indicate that the contribution of induced fission of various plutonium isotopes and other lighter elements is negligible. Only Pu^{242} has a spontaneous fission half-life com-

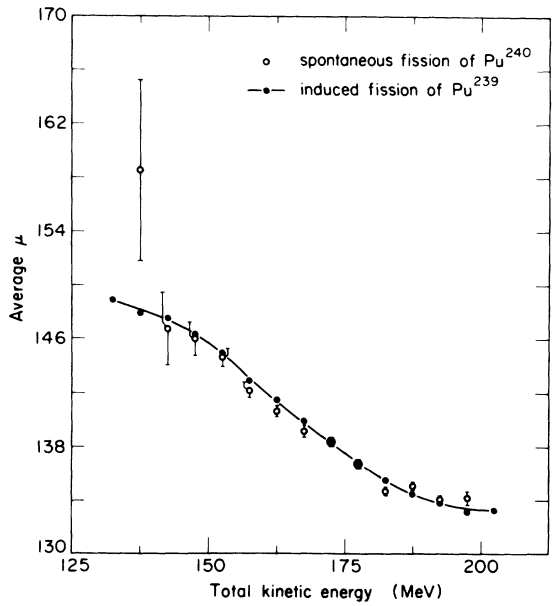

FIG. 7. Average heavy-fragment masses $\langle\mu_H\rangle$ for 5-MeV intervals of total kinetic energy for spontaneous fission of Pu^{240} and induced fission of Pu^{239} by beryllium-filtered neutrons. Smooth curves indicate quantities for the induced fission.

parable to that of Pu^{240}. However, its concentration is too small to affect the results significantly.

(2) The measured total kinetic energy distribution shows a secondary peak near 184 MeV. Data on spontaneous fission of transplutonium elements indicate that the average total kinetic energies released in the spontaneous fission of Cm^{244} and Cf^{252} lie in this region. The shape of the energy distribution suggests the possibility that the measured distribution might be a superposition of two independent symmetric energy distributions centered around two different average energy values. The analysis of the α spectrum from the target rules out the presence of Cm^{244} in any significant quantities. Because of the very small quantities of Cf^{252} (8×10^{-15} g of Cf^{252} compared with 3.2×10^{-5} g of Pu^{240}) required to produce the observed secondary peak in the energy distribution, and the relative rates of α emission, α spectrum analysis does not give conclusive evidence against Cf^{252} contamination. Therefore, an estimation of the fission events expected in the region near symmetric mass division, if a sufficient amount of Cf^{252} were present, was made. The actual yields in the symmetric region of the measured mass distribution indicate that Cf^{252} contribution to the measured fission events is also small. Comparison of the calculated and the measured fission rates also supports this conclusion. Discussion of these estimates is given in Appendix I.

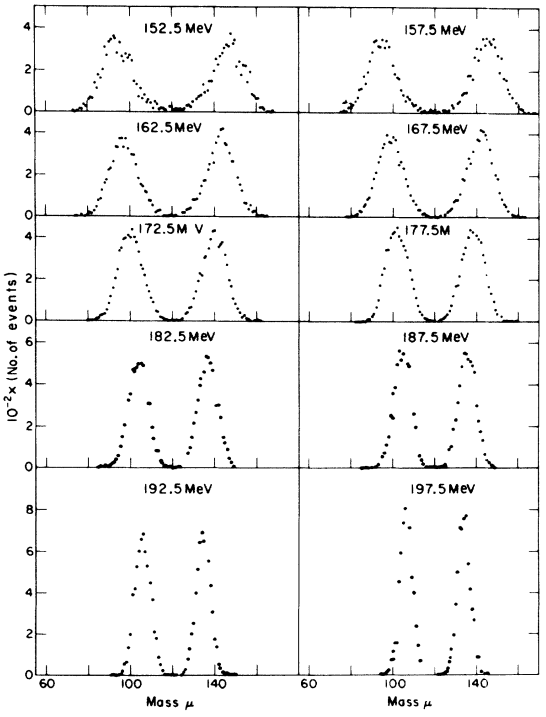

FIG. 8. Mass distributions $N(\mu)$ for the fission of Pu^{239} induced by beryllium-filtered neutrons obtained by considering fixed 5-MeV intervals of the total kinetic energy distribution. All curves are normalized to the distribution corresponding to interval centered at 172.5 MeV.

(3) The large α flux from the target may have produced nuclear reactions in the elements present in it, or a very small fraction of the decay products of various elements may be produced in the isomeric state instead of the ground state. All the fissionable isomeric states so far discovered are known to have half-lives less than a second, i.e., at least 10^{18} times smaller than the spontaneous-fission half-life of Pu^{240}. Therefore, only a very small amount of such nuclei in isomeric states is required. From the known α flux and number of nuclei of different elements present in the target, estimations of the cross section for the production of isomeric states were made. These estimations require a cross-section of the order of a barn, which is at least 10 times larger than the known cross sections for α particles of much higher energies. Therefore the possibility of contamination from the isomeric-state fission is excluded.

It is rather surprising to observe that the total kinetic energy in spontaneous fission is 3.7 MeV higher than in the neutron-induced fission of Pu^{239}. The compound nucleus Pu^{240} formed by addition of a slow neutron has $\approx$6.3-MeV excitation energy. Assuming that 0.12 neutrons/MeV of excitation energy[9] are emitted by the fragments, the increased neutron emission (2.83 neutrons compared with 2.12 from the spontaneous fission) accounts for 6 MeV. Thus, the higher average kinetic energy for the spontaneous fission implies reduced energy in γ emission.

Figure 8 shows the mass distributions for fixed total kinetic energy slices for the induced fission of Pu^{239}. The mass distributions become narrower and the yields in the symmetric region smaller with the increasing total kinetic energies. The higher average total kinetic energy and the narrower mass distribution for the spontaneous fission of Pu^{240} are in agreement with this trend. However, the shape of the mass distribution is distinctly different than that for the induced fission of Pu^{239}. The pair of detectors used for the induced-fission measurements was different than that used for the spontaneous-fission studies, and was calibrated by using another source. This may have introduced systematic errors in the absolute energy determinations but cannot change the shape of the mass distribution significantly.

The results of this work disagree significantly with the work of Mostovaya. She obtained a smooth mass distribution with a large value for the asym-

metric-to-symmetric fission ratio for the spontaneous fission of Pu^{240}. However, the value of the same ratio obtained by her for the thermal-neutron-induced fission of Pu^{239} is ≈ 20. All the recent data available indicate that this ratio must be much larger. Our value for this ratio (106) agrees better with the values of other workers. The smaller value of her ratio may be due to the poor resolution of the measurements. The solid-state detectors used in the present experiment have much better energy resolution than the ionization chamber used by Mostovaya. Still another possible explanation is the fact that she used a Po-α-Be neutron source and moderated the neutrons in the paraffin surrounding the fission chamber. The average energy of the neutrons from a Po-α-Be source is 4 MeV. Therefore, there may be a large contribution of fast neutrons to the measured induced-fission rate. For fast neutrons, the symmetric fission yield is known to be high. The energy difference of 1.5 ± 0.5 MeV based on her work therefore might not be the real difference between the spontaneous and the thermal-neutron-induced fission.

Our results indicate maximum fission yield for mass numbers 106 and 134. The radiochemical measurements of Laidler and Brown also show maximum yield for masses 105 and 133. However, nothing can be said from these radiochemical results about the secondary structure we observed at mass 144, as fission yields of only 3 isotopes were measured in this region. Figure 9 shows this radiochemical mass distribution superimposed on the $N(\mu)$ distribution of the present work.

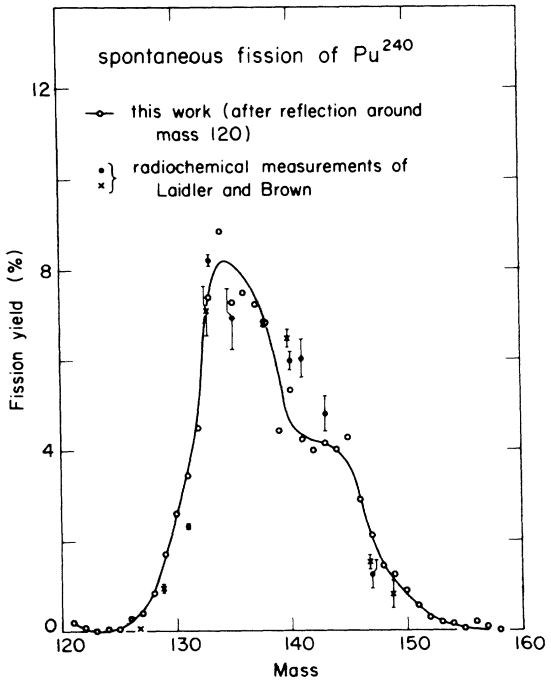

FIG. 9. Mass distribution $N(\mu)$ for spontaneous fission of Pu^{240} superimposed on the radiochemical mass distribution obtained by Laidler and Brown.

CONCLUSIONS

The results of the present measurements indicate that the shapes of the mass and kinetic energy distributions for the spontaneous fission of Pu^{240} differ significantly from those for the slow-neutron-induced fission of Pu^{239}.

Spontaneous fission was observed to give a higher average total kinetic energy, in apparent disagreement with other measurements. It is possible that the higher energy measured for the spontaneous fission is due to some systematic error introduced by the different sources used for the calibration of each pair of detectors. However, the differences in the shapes of various distributions will not be affected by this type of error in the absolute energy measurements.

ACKNOWLEDGMENTS

The authors are grateful to Dr. E. H. Kobisk of Oak Ridge National Laboratory for the preparation of the targets. The authors wish to thank Dr. Mary Derengowski for interest and help throughout the experiment.

APPENDIX I

Estimation of Effective Contamination

The total kinetic energy distribution for the spontaneous fission (Fig. 2) shows a secondary peak near 184 MeV and is wider than that for the induced fission of Pu^{239}. This shape of the energy distribution together with the higher value for the average total kinetic energy suggests that the measured distribution may be a superposition of two symmetric energy distributions centered around two different average energy values. Only contamination by transplutonium elements could contribute to the secondary peak as all fissionable elements lighter than plutonium have average total kinetic energy release less than 180 MeV.

Estimation of the amount of impurities that might be present was done in the following way by using the measured kinetic energy distribution. The spontaneous fission of Pu^{240} involves the ground state which has $J = 0^+$. Therefore the energy distribution might be the same as that for the induced fission of Pu^{239} from the $J = 0^+$ resonance level. Assuming this to be true, a symmetric energy distribution of width 28 MeV was drawn about the energy 173 MeV using the lower-energy side of

the measured distribution as a guide for its shape. This lower-energy side of the measured distribution should be comparatively free from the effects of the impurities. Figure 10 shows the results of such decomposition of $N(E_K)$ into two distributions. The difference appears like another total kinetic energy distribution of width 26.8 MeV centered around 187 MeV. The area under this curve is 33% of the total area under the $N(E_K)$ curve.

Consideration of half-lives indicates that only Cm^{244} and Cf^{252} need be considered. About 1.6×10^{-9} g of Cm^{244} or 8×10^{-15} g of Cf^{252} alone are needed to produce the observed effect. Cm^{244} contamination by this amount is possible only if the Pu^{240} sample contained some transplutonium elements (created during the production of Pu^{240}). The α spectrum analysis of the target indicates that if Cm^{244} is present, it must be at least 10 times smaller than required to produce the observed effect. It is not possible to draw any conclusions about the Cf^{252} contamination by this method, because of the relative proportions of Pu^{240} and Cf^{252}. The ratio of the α half-lives of Pu^{240} and Cf^{252} is 2580, while the ratio for spontaneous-fission half-lives is 1.85×10^{9}. Thus the contribution of Cf^{252} to the measured α-decay rate is very small compared with that to the fission events. Though the α energies of Cf^{252} and Pu^{240} differ by large amounts, estimation of Cf^{252} content made this way is not very reliable, because of the pileup problems due to the high Pu^{240} α-decay rate.

Estimation of the Cf^{252} contribution was made as follows: If Cf^{252} were really present in amounts indicated by the decomposition of the energy distribution, then the fission yields in the symmetric mass region would be modified. During the calibration of the detectors, Cf^{252} fission-fragment energies were measured under identical conditions. Analysis of the mass distribution was done by using these data. If Cf^{252} fission contributed to the data on Pu^{240} fission, these Cf^{252} events would be treated during the data analysis as if they were Pu^{240} events. Therefore, the Cf^{252} mass distribution was recalculated by using an appropriate scale factor (240/252). This mass distribution was then normalized so that the total of events in the distribution was 0.33 times the total of observed fission events. The normalized distribution was then subtracted from the real data. Figure 11 shows the resultant Pu^{240} mass distribution together with the measured mass distribution and the properly modified and normalized Cf^{252} distribution. The distribution for induced fission of Pu^{239}, normalized to the corrected Pu^{240} mass distribution is superimposed for comparison. Comparing the measured yields in the symmetric region with those expected if Cf^{252} were present in sufficient quantity, we conclude that Cf^{252} contamination, if any, is at least 5 times smaller than that needed to produce the observed effect. Note

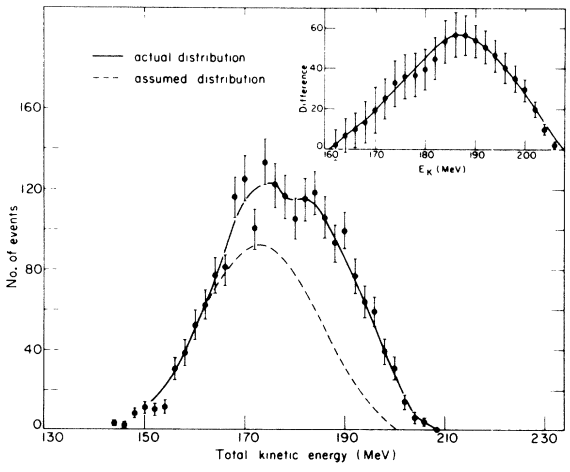

FIG. 10. Measured total kinetic energy distribution $N(E_K)$ for the spontaneous fission of Pu^{240} decomposed into two independent energy distributions. The dashed curve represents the assumed energy distribution for the spontaneous fission of Pu^{240}. The difference between the actual and the assumed distribution is shown in the inset.

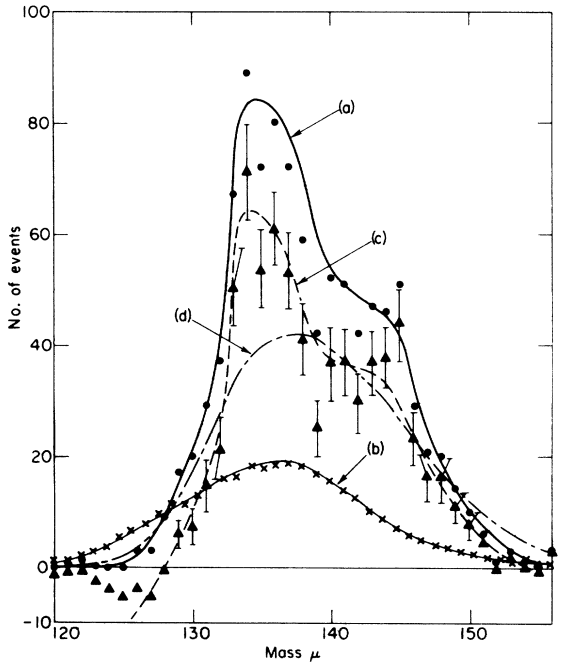

FIG. 11. Heavy-fragment mass distributions: (a) Measured Pu^{240} spontaneous-fission mass distribution (solid circles; (b) mass distribution due to Cf^{252} contamination if 33% of the total events were due to Cf^{252} (×'s); (c) corrected Pu^{240} mass distribution (triangles) obtained by subtraction of (b) from (a); and (d) mass distribution from Pu^{239} neutron-induced fission, normalized to corrected Pu^{240} distribution (smooth curve only).

also that the corrected Pu^{240} distribution still differs significantly from that for the induced-fission case. In particular, in the mass region 132–140, the Pu^{240} distribution is much higher than the one for induced fission. From Fig. 5 this is also the region where the largest amount of kinetic energy is released.

The amount of Pu^{240} in the sample was calculated by using the α-decay rate obtained after correction for contributions from other plutonium isotopes and Am^{241} (produced by the decay of Pu^{241}). The Pu^{240} spontaneous-fission rate calculated by using this value was 2.5 fissions/h, while the measured rate was 2.16 fissions/h. If Cf^{252} was present in significant amounts, the measured α-decay rate should change negligibly, but the fission rate should be 50% higher than the calculated one. This is another indication that the Cf^{252} contamination is negligible.

The above analysis leads us to believe that the observed structures in the mass and kinetic energy distributions were not produced by any contamination but are the true characteristics of the spontaneous fission of Pu^{240}.

†Work supported by the U.S. Atomic Energy Commission.

[1]W. J. Whitehouse and W. Galbraith, Phil. Mag. 41, 429 (1950).

[2]E. Segre and C. Wiegand, Phys. Rev. 94, 157 (1954).

[3]T. A. Mostovaya, in *Proceedings of the Second United Nations International Conference on the Peaceful Uses of Atomic Energy* (United Nations, Geneva, Switzerland, 1958), Vol. 15.

[4]V. N. Okolovich and G. N. Smirenkin, Zh. Eksperim. i Teor. Fiz. 43, 1861 (1962) [transl.: Soviet Phys.-JETP 16, 1313 (1963)].

[5]A. Smith, P. Fields, A. Friedman, S. Cox, and R. Sjoblom, in *Proceedings of the Second United Nations International Conference on the Peaceful Uses of Atomic Energy* (United Nations, Geneva, Switzerland, 1958), Vol. 15.

[6]J. B. Laidler and F. Brown, J. Inorg. Nucl. Chem. 24, 1485 (1962).

[7]J. Toraskar and E. Melkonian, Phys. Rev. C 4, 267 (1971).

[8]H. W. Schmitt, J. H. Neiler, and F. J. Walter, Phys. Rev. 141, 1146 (1966).

[9]B. C. Diven and J. C. Hopkins, in *Proceedings of the Seminar on the Physics of Fast and Intermediate Reactors, Vienna, Austria, 1961* (International Atomic Energy Agency, Vienna, Austria, 1962) Vol. 1, p. 149.

PHYSICAL REVIEW C VOLUME 4, NUMBER 4 OCTOBER 1971

Neutron-Hole-State Structure in $N = 81$ Nuclei. II. ^{140}Ce and ^{138}Ba(p, d)†

R. K. Jolly and E. Kashy

Cyclotron Laboratory, Michigan State University, East Lansing, Michigan 48823

(Received 5 May 1971)

In continuation of our program of neutron-hole-state studies in $N = 81$ nuclei, angular distributions of deuterons from (p,d) reactions (energy resolution ~35 keV) on ^{140}Ce and ^{138}Ba at $E_p = 35$ MeV have been measured and compared with distorted-wave Born-approximation calculations including finite-range and nonlocality corrections. These calculations yield acceptable spectroscopic factors and are in fair agreement with the shapes of the experimental angular distributions. The neutron-single-hole energies have been determined. These energies (in MeV) are $d_{3/2}$, 0.0; $s_{1/2}$, 0.33; $h_{11/2}$, 1.07; $d_{5/2}$, 1.72; and $g_{7/2}$, 2.90 for ^{139}Ce; and $d_{3/2}$, 0.0; $s_{1/2}$, 0.54; $h_{11/2}$, 1.07; $d_{5/2}$, 1.71; and $g_{7/2}$, 2.93 for ^{137}Ba.

Considerable fractionation of the $(2d_{5/2})_\nu^{-1}$ and the $(1g_{7/2})_\nu^{-1}$ states is observed while the $(1h_{11/2})_\nu^{-1}$ and the $(3s_{1/2})_\nu^{-1}$ states are each observed to split mostly into two components. Systematics of the energies and strengths of the various neutron-single-hole states and their components are presented for all $N = 81$ nuclei from ^{137}Ba through ^{143}Sm and the significance of the systematics discussed. No measurable population of any neutron state in the $82 < N \leq 126$ major shell has been observed.

I. INTRODUCTION

In a previous paper[1] (henceforth referred to as Paper I) we reported our results on the analysis of (p, d) measurements on the $N = 82$ nuclei of ^{144}Sm and ^{142}Nd[1] together with a study of the effects of different values of lower cutoff, finite-range and nonlocality (FRNL) corrections, and density dependence of the effective pn interaction on the shapes and magnitudes of distorted-wave Born-approxima-